第 20 卷 第 6 期 强 激 光 与 粒 子 束 Vol. 20, No. 6
2008 年 6 月 HIGH POWER LASER AND PARTICLE BEAMS Jun., 2008

Article ID: 1001-4322(2008)06-0951-05

Characteristics of transient collisional excited Ni-like Ag 13.9 nm XRL driven by two picosecond pulses*

QIAO Xiu-mei, ZHANG Guo-ping

(*Institute of Applied Physics and Computational Mathematics*, *P.O. Box* 8009, *Beijing* 100088, *China*)

Abstract: The transient collisional excited Ni-like Ag 13.9 nm X-ray laser was simulated. Driven by two picosecond short pulses preceded by a 330 ps long prepulse, different short pulses of 1 ps, 2 ps and 3 ps were considered and for each case the angular characteristics of the output X-ray laser are presented in this paper. Detailed analysis shows that the (330 ps, 1 ps, 1 ps) pumping combinations delayed by about 500 ps can extract higher gains near critical surface and it works best. To get the effect of the first short pulse, X-ray lasers driven by only one short pulse following the same long prepulse was simulated and optimization was made. By comparing the optimized case of the two pumping scheme, the advantages of the two short pulses pumping scheme was indicated.

Key words: X-ray laser; Transient collisional excitation; Gain; Ni-like Ag

CLC number: TN241 **Document code**: A

One of the goals for X-ray laser study is to get saturated operation of X-ray laser at water-window wavelength, and the promising candidate is Ni-like X-ray lasers of high Z target. The transient collisional excited (TCE) scheme sharply reduces the driving energy and saturated operation of X-ray laser with wavelength up to 12 nm has been obtained with only ~10 J energy[1-6]. As the pumping intensity is proportional to $\lambda^{-9/2}$, λ is the wavelength of X-ray laser, with further decrease of wavelength of X-ray laser, more pumping energy is needed to produce properly ionized plasma. For example, the Ni-like Sm 7.3 nm TCE X-ray laser needs more than 50 J energy[7]. The recent TCE Ni-like Ag 13.9 nm X-ray laser experiment driven by a single picosecond pulse[8-10] suggests a new pumping scheme, in which a low-level pedestal prepulse produces lowly ionized preplasma with low electron temperature, while, instead of merely heating the plasma, the picosecond short pulse heats and ionizes the preplasma to Ni- or Ne-like states. The new pumping scheme seems useful for realization of water-window TCE X-ray laser, because the high pumping intensity could be easily realized by the picosecond short pulse. The Ni-like Ag 13.9 nm X-ray laser driven by two picosecond short pulses following a low-level prepulse has been demonstrated experimentally[6]. Characteristics of X-ray laser produced by this method could be studied by properly designing the pumping condition[11]. However, as the TCE Ni-like Ta X-ray laser experiment is not available yet, we study the characteristics of Ni-like Ag 13.9 nm X-ray laser driven by the new scheme instead.

1 Simulation results

1.1 Preplasma status

The Ni-like Ag 13.9 nm TCE X-ray laser is driven by two picosecond short pulses preceded by a 330 ps long pulse. The peak to peak separation time dt_{21} between the long pulse and the first short pulse is 2.16 ns, and the second main short pulse is delayed by the varying time dt_{23}. The pulse energies are 0.30 J, 0.15 J and 2.50 J respectively. The focus line is 0.6 cm long and 50 μm wide. And the traveling wave pumping could be adopted using a step mirror. All the three pulses are Gaussian with a wavelength of 1.053 μm.

* **Received date**: 2007-10-16; **Revised date**: 2008-02-21
Foundation item: supported by National High-Tech Research and Development Plan
Biography: Qiao Xiumei(1976 —), female, Ph. D., engaged in theoretical study of X-ray Laser; xiumeiq123@163.com。

The low-level 330 ps long prepulse produces a small volume of plasma and after 2.16 ns expansion, the first picosecond short pulse comes and excites a shock wave in plasma. As the plasma keeps on expanding, the intensity of the shock wave gradually decreases and a flat region with small electron density gradient ∇N_e is produced as shown in Fig. 1. By choosing proper dt_{23}, the flat region could work as the gain region, which can increase the absorption of the second short pulse energy and benefit the amplification of X-ray laser.

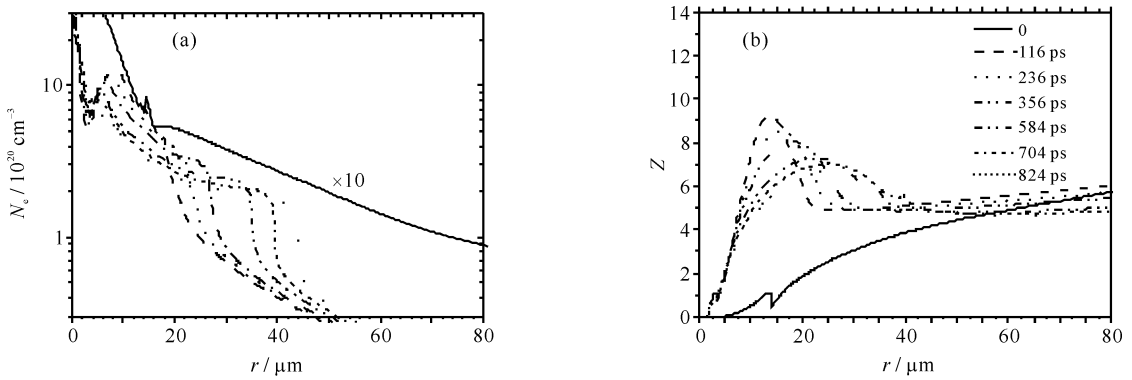

Fig. 1 Time evolution of pre-plasma status: (a) electron density N_e; (b) average ionization Z *vs* distance from target surface r in μm for different time. The long prepulse is 330 ps with 0.3 J energy, and the short pulse is 1 ps with 0.15 J energy. 0 ps is set at the peak time of the first short pulse

Fig. 1 shows the time evolution of electron density N_e in 10^{22} cm^{-3} (a) and the average ionization Z (b) versus the distance from the target surface r in μm, simulated by the 1.5 dimensional hydrodynamic code JB19. Except for special indication, the long prepulse in the simulation is 330 ps with 0.3 J energy, 0 ps is the peak time of the first short pulse, and dt_{21} is 2.16 ns. The first short pulse here is 1 ps with 0.15 J energy. Fig. 1 shows that a quite flat region appears on the curve for N_e with average value larger than 2×10^{20} cm^{-3}, and it ends with a steep fall at the outer end, indicating that the pumping energy deposits into the gain region, which is beneficial. And a very similar region is also found in experiment. We have also considered 2 ps and 3 ps short pulses with the same energy, and simulation indicates that when the short pulse is longer, N_e in the flat region is slightly smaller if dt_{23} is the same.

1.2 Simulation results

To obtain the optimized results, we have considered (330 ps, 1 ps, 1 ps), (330 ps, 2 ps, 2 ps) and (330 ps, 3 ps, 3 ps) pumping combinations at the same conditions except various dt_{23}, which we call model Ⅰ, model Ⅱ and model Ⅲ, respectively. For each model we presents the small signal gain g in cm^{-1} based on Linford formula[12] versus dt_{23} in Fig. 2. It is shown that in each model, g increases with the decrease of dt_{23}, as shorter dt_{23} causes larger Ne in preplasma, N_e in the gain region will be larger. But on the other hand, if dt_{23} is very short, the picosecond short pulse can not propagate into the deep inside of the flat region, but deposit its energy in the outside region, the shape of N_e will be severely destroyed, which is harmful to the propagation of X-ray laser. Fig. 2 also indicates that under fixed dt_{23}, model Ⅰ has the largest g, which could be attributed to the higher N_e in pre-plasma produced as mentioned above. We are interested in the quality of the output X-ray laser, Fig. 3 shows the divergence angle θ in mrad of the output X-ray laser for model Ⅰ, model Ⅱ and model Ⅲ versus dt_{23} in ps. It tells us that with the decrease of dt_{23}, θ first falls slightly and then rises to a relatively larger value after obtaining the minimum value for the three models. The minimum value in model Ⅰ is much smaller than those in model Ⅱ and model Ⅲ. Fig. 4 (a) shows the angular distribution of the output intensity for model Ⅰ, model Ⅱ, and model Ⅲ with dt_{23} of 500 ps, 600 ps and 500 ps. The intensities in the latter two models are multiplied by 15 and 50, respectively. And a sharp single peak appears at about 7.74 mrad in model Ⅰ, while in model Ⅱ and model Ⅲ, two peaks appear, which accounts for the large θ observed in Fig. 3. In the following text, we will take model Ⅰ with dt_{23} of 500 ps as an example to illustrate the reason for the above differences.

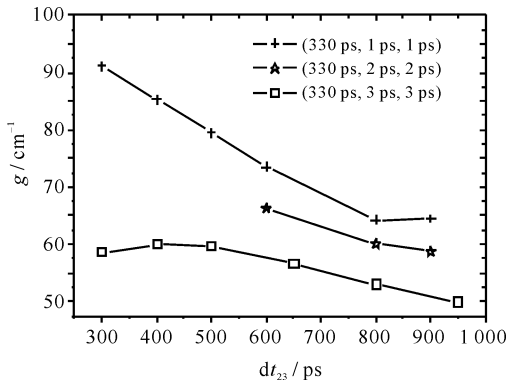

Fig. 2 Small signal gain g in cm^{-1} *vs* dt_{23} in ps for the three models. The target length is 0.3 cm

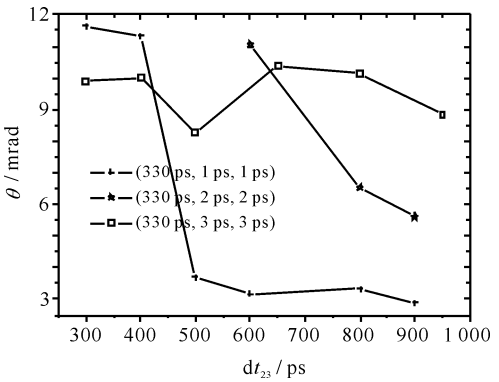

Fig. 3 Divergence angle θ in mrad of the output X-ray laser *vs* dt_{23} for the three models. The target length is 0.3 cm

Fig. 4 (a) shows the time evolution of local gain G in cm^{-1} versus r for model Ⅰ with dt_{23} of 500 ps. It is shown that high G first appears in a small narrow region near critical surface, and as time goes on, the plasma in this region is over-ionized to Co-like ions, while more plasma outside is properly ionized, hence the peak gain G_p moves outward. The variance of N_e as a function of r, has little change within the short time of amplification, it can be referred to the open circle in Fig. 5 (a). A flat region with average value larger than 6×10^{20} cm^{-3} in the open circle curve is observed, N_e near critical surface, however, still varies quite steeply. The time evolution of G combining with the variance of N_e versus r, suggests that two regions contribute to the amplification, one is the inner region near critical surface with large ∇N_e of $\sim -5.85\times10^{23}$ cm^{-4}, the other locates in the flat region with small ∇N_e of $\sim 1.10\times10^{23}$ cm^{-4}. According to refraction law for the laser line, the X-ray laser line is deflected by ~ 8.78 μm and ~ 1.65 μm respectively after propagating 0.15 cm length in the above two regions in the gain region. In the former region, it starts propagating with large negative angle into the deep inside of the gain region and leaves with a large positive angle, whereas in the latter region, it starts with a small negative angle or even with positive angle, and leaves with a small positive angle. Thus the former gain region is responsible to the peak at large refraction angle ϕ, while the latter to the peak at small ϕ, and the cooperation of the two regions produces the large divergence angle observed in Fig. 3.

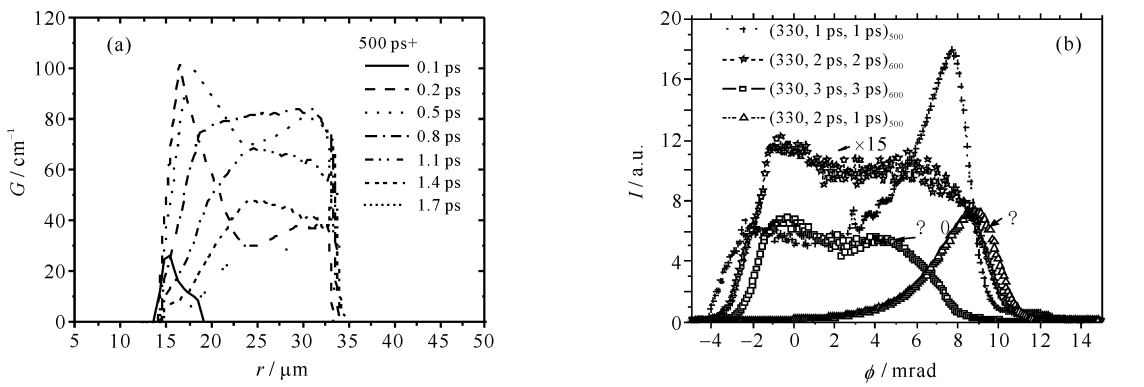

Fig. 4 (a) time evolution of G in cm^{-1} *vs* r in μm, 0 μm is position of the initial target surface.
(b) Distribution of output intensity I in arbitrary unit as function of refraction angle ϕ in mrad for model Ⅰ with $dt_{23}=500$ ps, model Ⅱ with $dt_{23}=600$ ps, and model Ⅲ with $dt_{23}=500$ ps.
I in model Ⅱ and model Ⅲ is multiplied by 15 and 50, respectively. 0 ps is the peak time of the first short pulse

To test the above analysis, in model Ⅱ with $dt_{23}=600$ ps, the 2 ps short main pulse was replaced by a 1 ps short pulse with the same energy, making electron temperature T_e and abundance of Ne-like ion near critical surface better matched, and the simulated final g is ~ 69.78 cm^{-1}, and the angular distribution of output intensity is plotted in Fig. 4 (b) by the open triangle and it is multiplied by 3. The single peak at $\sim$ 8.78 mrad on the open triangle line suggests that the contribution of the inner region near critical surface predominates that of the flat region resulting in a very small θ of ~ 3.35 mrad.

To get the effect of the first short pulse, we have modeled X-ray lasers driven by only one short pulse preceded by the same long prepulse, and optimization versus short pulse length and peak to peak separation time was made to find the optimized pumping pulse of a ~3 ps short pulse delayed by ~1 ns (model Ⅳ), and the g obtained is only ~50 cm^{-1}, and θ and ϕ are ~6.93 mrad and ~3.1 mrad respectively. Fig. 5 shows the plasma status when the output intensity peaks, Fig. 5 (a) is for model Ⅰ at 0.5 ps after the peak time of the second short pulse, and Fig. 5 (b) is for model Ⅳ at 2.2 ps after the peak time of the short pulse. Compared to model Ⅳ, model Ⅰ has the following characteristics: First, it has much wider gain region than model Ⅳ (the full width at half maximum (FWHM) of G is ~20 μm and ~5 μm, respectively); secondly, its N_e in the gain region is larger, with average value larger than ~6×10^{20} cm^{-3}, while in model IV, it is less than ~5×10^{20} cm^{-3}; thirdly, its N_e in the gain region varies very gently, whereas in model IV, it varies steeply. The narrow gain region together with steeply varying N_e in model IV severely limits the amplification near critical surface where higher G appears at earlier time, thus the gain region that contributes most is the under-dense region with N_e less than ~5×10^{20} cm^{-3}, which can partly account for the optimized short pulse length of 3~4 ps instead of ~1 ps.

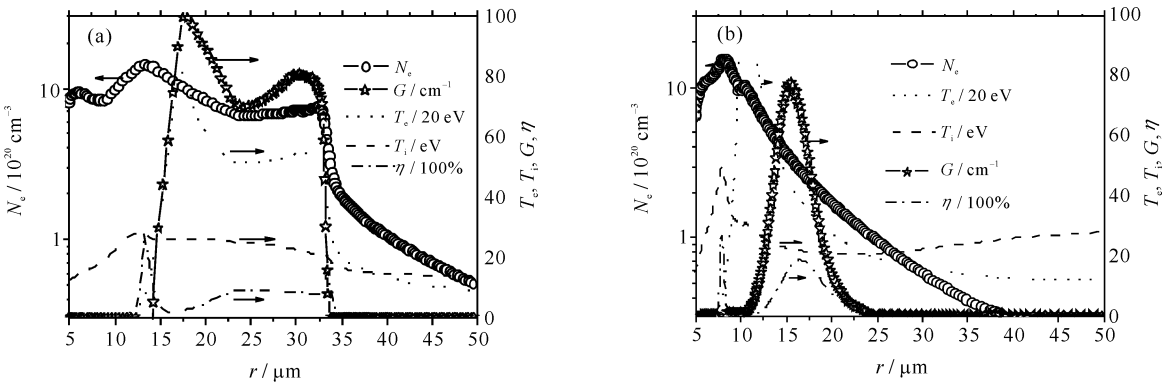

Fig. 5 N_e, T_e in 20 eV and T_i temperature in eV, abundance of Ni-like ions η in 100% in unit and G in cm^{-1}.
(a) model Ⅰ, 0.5 ps after the peak time of the second short pulse; (b) model Ⅳ, 2.2 ps after peak time of the short pulse

2 Discussion

Ni-like Ag 13.9 nm X-ray laser driven by two ps short pulses preceded by a 330 ps long pulse is simulated by our code series. Models using two 1 ps, 2 ps and 3 ps short pulses at the same energy are considered. It is found that the 1 ps model gives larger g than the 2 ps model or the 3 ps model. For each model, optimization versus dt_{23} is made and for the three optimized pumping conditions, angular characteristics of the output X-ray laser are presented. Detailed analysis to the ray-trace of X-ray laser show that two regions contribute to the amplification of the X-ray laser, one is near critical surface with large ∇N_e, the other is the flat region in the under-dense region, and the cooperation of the two regions produces a large θ. To get a small θ, the contribution of the former region should predominate that of the latter one, so that we should carefully choose the length of the second short pulse and dt_{23}. In this sense, model (330 ps,1 ps,1 ps) with dt_{23} of ~500 ps or ~600 ps can extract higher G near critical surface and it works best.

In order to observe the effect of the first short pulse, X-ray laser driven by only one short pulse preceded by the same long prepulse was simulated and optimized. Simulation indicates that the optimized short pulse is ~3 ps delayed by about 1 ns (model Ⅳ). Comparing the two optimized models, it is found that model (330 ps, 1 ps, 1 ps) has the following advantages: firstly, it produces wider gain region of ~20 μm, larger than only ~ 5 μm in model Ⅳ and secondly, it produces smooth varying N_e in gain region, and thus high G near critical surface can be extracted.

Acknowlegement The authors thank the Atomic Group of IAPCM for their atomic data. And thank the coworkers in High Computation Center of IAPCM for the convenience they offered.

References:

[1] Nickles P V, Shlyaptsev V N, Kalachnikov M, et al. Short pulse X-ray laser at 32.6 nm based on transient gain in Ne-like titanium[J]. *Phys Rev Lett*, 1997, **78**:2748-2751.

[2] Dunn J, Osterheld A L, Shepherd R, et al. Demonstration of X-ray amplification in transient gain nickel-like palladium scheme[J]. *Phys Rev Lett*, 1998, **78**: 2825-2828.

[3] Ozaki T, Ganeev R A, Lshizawa A, et al. Highly directively 18.9 nm nickel-like molybdenum X-ray laser operating at 150 mJ pumping energy[J]. *Phys Rev Lett*, 2002, **89**:**253902**.

[4] Dunn J, Osterheld A L, Nilsen J, et al. Gain saturation regime for laser-driven tabletop, transient Ni-like ion X-ray lasers[J]. *Phys Rev Lett*, 2000, **84**:4834-4837.

[5] Nilsen J, Li Y, Dunn J. Modeling picosecond-laser-driven neonlike titanium X-ray laser experiments[J]. *J Opt Soc Am B*, 2000, **17**:1084-1092.

[6] Kawachi T, Kado M, Tanaka M, et al. Gain saturation of nickel-like silver and tin X-ray lasers by use of a tabletop pumping laser system [J]. *Phys Rev A*, 2002, **66**:**033815**.

[7] King R E, Pert G J, McCabe S P, et al. Saturated X-ray lasers at 19.0 nm and 7.3 nm pumped by a picosecond traveling-wave excitation [J]. *Phys Rev A*, 2001, **64**:**053810**.

[8] Janulewicz K A, Lucianetti A, Priebe G, et al. Saturated Ni-like Ag X-ray laser at 13.9 nm pumped by a single picosecond laser[J]. *Pulse Phys Rev A*, 2003, **68**:**051802**.

[9] Janulewicz K A, Lucianetti A, Priebe G, et al. A tabletop collisional Ni-like Ag X-ray laser at 13.9 nm pumped by single picosecond laser pulse[C]//Proc of the 8th on X-ray lasers. 2002:26-30.

[10] Janulewicz K A, Nickles P V, King R E, et al. Influence of pump pulse structure on a transient collisionally pumped Ni-like Ag X-ray laser [J]. *Phys Rev A*, 2004, **70**:**013804**.

[11] Qiao X M, Zhang G P. Theoretical Study of Ni-like Ag 13.9 nm TCE X-ray laser driven by two picosecond pulses[J]. *Chin Phys*, 2007, **16**(5):1370-1373.

[12] Linford G J, Peressini E R, Soody W R, et al. Very long lasers[J]. *Appl Opt*, 1974, **13**:379-390.

双短脉冲驱动的瞬态电子碰撞激发类镍银 13.9 nm X 光激光

乔秀梅, 张国平

(北京应用物理与计算数学研究所, 北京 100088)

摘 要: 研究了两个皮秒短脉冲驱动的瞬态电子碰撞激发类镍银 13.9 nm X 光激光,考察了脉宽分别为 1,2,3 ps 驱动的情况,分别给出了输出 X 光激光的角分布特性。模拟表明,(330 ps, 1 ps, 1 ps)驱动条件下,第二短脉冲延迟约 500 ps,可以充分利用临界面附近的高增益。通过与相同长脉冲条件下单短脉冲驱动的结果相比较,分析了第一个短脉冲的作用及双脉冲驱动的优点。

关键词: X 光激光; 瞬态碰撞激发; 增益; 类镍银